

**OPTIMIZATION OF TROPOSPHERIC DELAY MAPPING FUNCTION
PERFORMANCE FOR HIGH-PRECISION
GEODETTIC APPLICATIONS[†]**

Virgílio B. MENDES^{1,2} and Richard B. LANGLEY²

¹Faculty of Sciences of the University of Lisbon, R. Ernesto de Vasconcelos, Bloco C1, Piso 3, 1700 Lisboa, Portugal; e-mail: vmendes@lmc.fc.ul.pt. ²Geodetic Research Laboratory, Department of Geodesy and Geomatics Engineering, University of New Brunswick, P.O. Box 4400, Fredericton, N.B., E3B 5A3 Canada; e-mail: lang@unb.ca.

ABSTRACT – *The propagation delay induced by the electrically neutral atmosphere, commonly known as the tropospheric delay, is one of the most difficult-to-model errors affecting space geodetic techniques. An unmodeled tropospheric delay affects mainly the height component of position and constitutes therefore a matter of concern in space-geodesy applications, such as sea-level monitoring, postglacial rebound measurement, earthquake-hazard mitigation, and tectonic-plate-margin deformation studies.*

The tropospheric delay is commonly divided into two components, “hydrostatic” and “wet”, each one consisting of the product of the delay at the zenith and a mapping function that projects the zenith delay to the desired line-of-sight. In general, these mapping functions are parameterized by specific meteorological or other site-dependent parameters that can be readily determined. Other functions require parameters that describe the temperature profile for a given location and time, such as tropopause height and temperature lapse rate, which are in general not available. In such cases, nominal values for these parameters are used.

We have evaluated the performance of three temperature-profile-dependent mapping functions developed by the Harvard-Smithsonian Center for Astrophysics (CfA), the Jet Propulsion Laboratory (Lanyi) and the Shanghai Observatory (UNSW931) under different parameterization settings, using ray traces of a one-year dataset of radiosonde profiles from 50 stations distributed worldwide. Ray tracing was performed for 6 different elevation angles, starting at 3 degrees. The different parameterizations included the use of nominal values, monthly means for each station, and values obtained from two simple models we have developed. For the Lanyi mapping function, a total of six different parameterizations were evaluated. We conclude that the use of nominal parameter values yields significant errors in the mapping function performance, which are largely correlated with the station latitude. Using our models for tropopause height and lapse rate determination, we were able to optimize the CfA and UNSW931 functions by significantly reducing the r.m.s. scatter about the mean. The improvement for Lanyi is also notable compared with the parameterization using default values, but only marginal if compared with the solution using monthly means.

[†]Proceedings of DORIS Days, 27-29 April 1998, Toulouse, France.

1. INTRODUCTION

When traveling through the electrically-neutral atmosphere, radio signals used by radiometric techniques are affected by the variability of the refractive index, causing an excess path delay and ray bending. The effect is commonly known as tropospheric propagation delay (or simply tropospheric delay), even though this designation is misleading, as the stratosphere has a significant contribution to the total delay. The tropospheric delay is difficult to fully correct and constitutes one of the major residual error sources in modern space geodetic techniques – such as DORIS (Doppler Orbitography and Radiopositioning Integrated by Satellite), GPS (Global Positioning System) and VLBI (very long baseline interferometry) – affecting mainly the estimates of the height component of position. The improvement in tropospheric delay modeling is therefore essential in applications such as sea-level monitoring, postglacial rebound measurement, earthquake-hazard mitigation, and tectonic-plate-margin deformation studies, where the highest possible position accuracy is sought.

The tropospheric delay is conveniently expressed as the contribution of a hydrostatic component, due mostly to dry molecular constituents of the atmosphere, and a wet component, associated with the water vapor in the atmosphere. Moreover, each of these components can be expressed as the product of the delay experienced by the radio signals in the zenith direction, the zenith delay, and a mapping function, which models the elevation angle dependence of the tropospheric delay:

$$d_{\text{trop}} = d_{\text{h}}^z m_{\text{h}}(\epsilon) + d_{\text{w}}^z m_{\text{w}}(\epsilon), \quad (1)$$

where d_{trop} is the tropospheric delay at a given elevation angle ϵ , d_{h}^z and d_{w}^z are, respectively, the hydrostatic and wet zenith delays, and $m_{\text{h}}(\epsilon)$ and $m_{\text{w}}(\epsilon)$ are the hydrostatic and wet mapping functions, respectively.

Most of the existing mapping functions used in modeling the elevation dependence of the neutral-atmosphere propagation delay are generally driven by values of readily-available meteorological parameters, such as surface pressure and temperature. In order to better describe the variations of the propagation delay for a particular site and season, more sophisticated mapping functions (such as the ones developed by Lanyi [Lany 84], Davis et al. [Davi 85], and Yan and Ping [Yanp 95]) require some additional information about the temperature profile, namely the tropopause height (H_t) and the temperature lapse rate (λ). In most situations, this information is not available and nominal global values are used. A better determination of these parameters is essential to take advantage of the “tuning” capability of these mapping functions for different locations, as we will demonstrate.

2. TEMPERATURE PROFILE PARAMETERS

Traditionally, the tropopause is defined as the boundary between the troposphere and the stratosphere, characterized by a discontinuity in the temperature gradient. The World Meteorological Organization established a more refined definition (see, for example, [Met 91]), which is the basis of the tropopause heights reported in radiosonde data archives. Based on data from different sources, we have established a database of ~51 500 tropopause heights, corresponding to one-year (1992) determinations for 100 radiosonde stations distributed around the world. The mean global value obtained from this database was $11.3 \text{ km} \pm 2.6 \text{ km}$, a value very similar to the one suggested by Davis et al. [Davi 85], that is, 11.231 km. The large standard deviation associated with our mean value reflects the large latitudinal and seasonal variations of this parameter, confirmed by the contour plots for just the North American region shown in Fig. 1. The triangles identify the locations of the radiosonde stations used in the analysis.

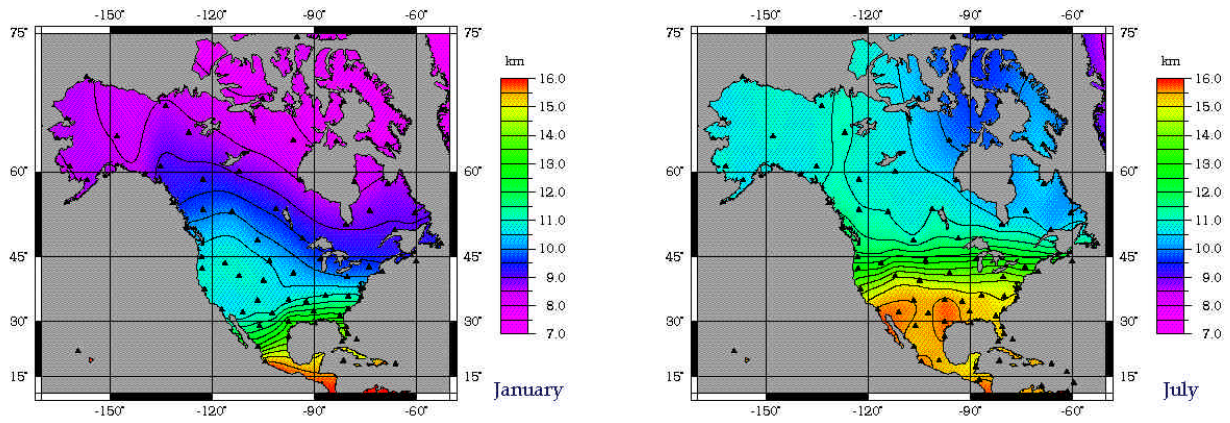


Fig. 1 – Tropopause height distribution for North America in January and July (1992).

These plots show that the latitudinal and seasonal variations of the tropopause height are quite large and can not be accounted for by using a single nominal value. The tropopause reaches the highest values at low latitudes, with very small seasonal variation. The minimum values are observed at high latitudes. Large seasonal variations are observed at both middle and high latitudes. A more detailed analysis revealed that the tropopause height is well correlated with the surface temperature and we were able to establish a model expressing this dependence:

$$H_t \text{ (km)} = 7.508 + 2.421 \exp \frac{t_s}{22.90} , \quad (2)$$

where t_s is the surface temperature, in °C. The details of model development are described by Mendes [Mend 98].

The temperature lapse rate also varies significantly both in time and space. In our terminology, we define lapse rate () as the negative rate of change of temperature with height (H):

$$= - \frac{dT}{dH} . \quad (3)$$

The sign is conventionally chosen so that the lapse rate is positive when the temperature decreases with height (as it normally does in the troposphere). Based on a one-year radiosonde dataset from 100 stations, we have determined ~62 500 values of mean temperature lapse rates within the troposphere (defined as the slope of the straight line that best fits the temperature profile of radiosonde soundings, computed between the top of the inversion layer and the tropopause height). The mean global value for this database was 6.17 K/km \pm 0.82 K/km, which is lower than the commonly used 6.5 K/km, a value closer to the mean temperature lapse rate observed in tropical regions. We have concluded that the lapse rate shows large seasonal variations at continental stations with cold winters, and reaches the maximum values in mid-latitude arid regions, as portrayed for North America, as an example, in Fig. 2. The minimum values are again observed at high latitudes. We have also found that there is a correlation between the temperature lapse rate and the surface temperature (although weaker than that detected for the tropopause height), which is the basis of the model we have developed:

$$(\text{°C} / \text{km}) = 5.930 + 0.0359 t_s . \quad (4)$$

Again, details on this model can be found in Mendes [Mend 98].

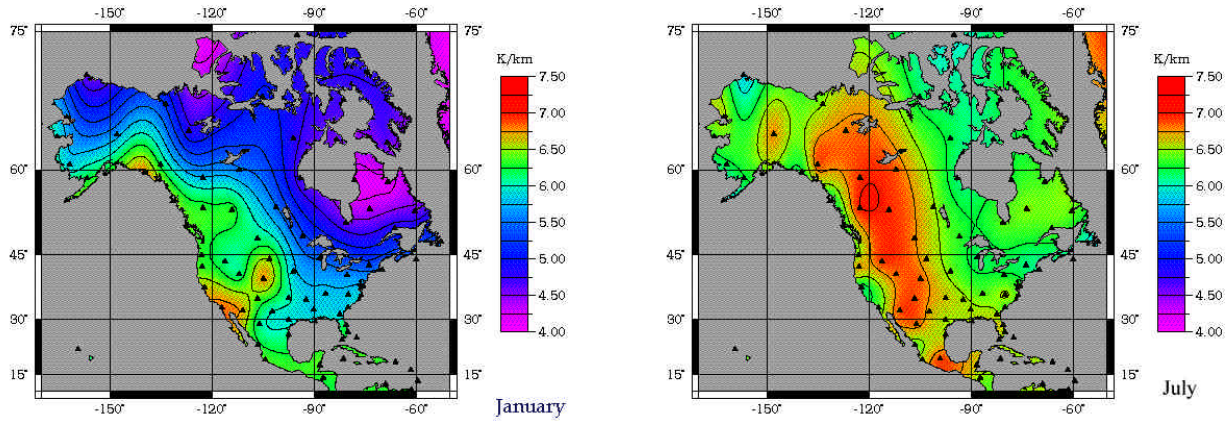


Fig. 2 – Temperature lapse rate distribution for North America in January and July (1992).

In addition to the development of models, we have also computed mean monthly values of tropopause heights and lapse rates for each of the radiosonde stations. The performance of the mapping functions driven by these parameters has been used as our main reference against which other strategies are compared.

3. MAPPING FUNCTION PARAMETERIZATION

There are at present three mapping functions that can readily use, as part of their parameterization, site-specific parameters relating to the temperature profile.

The most complex mapping function in use was developed by Lanyi at the Jet Propulsion Laboratory [Lany 84]. The Lanyi mapping function, which maps both components of the zenith delay, was developed using a semi-analytical approach and fitted for elevation angles above 6° . It uses three-linear section temperature profiles. The neutral-atmosphere propagation delay is expanded up to the third order in refractivity, where the second and third order terms describe the bending effect. Latitude and site-dependent variations with respect to an average profile can be modeled through inputs of tropopause height, inversion height (H_i), and temperature lapse rate.

The hydrostatic mapping function developed at the Harvard-Smithsonian Center for Astrophysics [Davi 85], also known as CfA-2.2 (hereafter CfA) is based on the continued fraction form of Marini [Mari 72]. The coefficients of the CfA mapping function were obtained from ray tracing through idealized model atmospheres, down to 5° elevation angle, and are expressed as linear functions of departures with respect to nominal values of surface temperature, total pressure, partial water vapor pressure, temperature lapse rate, and height of the tropopause. Even though this mapping function was developed for mapping the hydrostatic zenith delay only, it can also be used for the wet delay. This procedure introduces a “small” error, of uncertain magnitude [Davi 85].

Two mapping functions were developed by Yan and Ping at the Shanghai Observatory, both based on the continued expression of the complementary error function [Yanp 95]. One of these functions is based on atmospheric profiles provided by CfA and other standard atmospheric parameters and was labeled UNSW931 (UNSW, in this paper). The other mapping function is based on the atmospheric profile given by Hopfield [Hopf 69] and is not considered in this analysis. The UNSW mapping function is driven by the same parameters as is CfA and was fitted to elevation angles above 2.5° . Although not specified explicitly, we assume that UNSW should only be applied to map the hydrostatic component; under this assumption, and as in the case of CfA, mapping the wet zenith delay with UNSW will therefore introduce an error.

The CfA and UNSW mapping functions were tested under three different settings for tropopause height and lapse rate: a) monthly means for each radiosonde station (CfA1, UNSW1); b) global default values suggested by the authors, 11.231 km and 6.5 K km^{-1} (CfA2, UNSW2); c) our models (CfA3, UNSW3).

The Lanyi mapping function was tested using six different parameter settings, as follows: a) mapping function driven by all the nominal default values suggested by Lanyi [Lany 84] (LA1); b) temperature profile parameters (surface temperature, lapse rate, and tropopause height) computed according to an interpolation scheme through the U.S. Standard Atmosphere Supplements, 1966 [Envi 66], as recommended by Sovers and Jacobs [Sove 96]. The estimated temperature profile parameters corresponding to each of the model atmospheres are presented in Table 1.

Table1 – U.S. Standard Atmosphere Supplements profile parameters [Sove 96].

Date	ϕ (°)	T (K)	α (K/km)	H_i (km)	H_t (km)
January 28	15	300.940	6.33961	0	13.7889
	30	291.642	6.19987	0	12.1382
	45	275.593	5.43813	0	9.83468
	60	266.007	5.37249	0	8.51284
	75	256.212	4.21860	0	11.5115
July 28	15	300.940	6.33961	0	13.7889
	30	301.074	6.14791	0	13.6649
	45	296.381	6.01369	0	12.6266
	60	288.455	5.93926	0	9.67076
	75	283.577	5.84173	0	9.50090

These parameters are subsequently linearly interpolated to match the latitude and height of the station of interest, and finally interpolated to the appropriate day of year, using a sinusoid with extrema in January and July (the southern hemisphere is considered to be half a year out of phase with respect to the northern hemisphere). The inversion height in this version is set to zero (LA2); c) mean monthly values for the inversion height, tropopause height and lapse rate of our databases, coupled with the observed surface temperature and pressure (LA3); d) same as strategy c), but with mean monthly values of surface temperature at every radiosonde station (LA4); this strategy avoids the use of the actual surface temperature and the values used are a better representation of the average temperature of the surface layer, as required by the mapping function; e) mean monthly values of temperature of our database, coupled with the global values of lapse rate and tropopause height suggested by Davis et al. [Davi 85] (LA5). As in strategy b), the observed pressure was used and the inversion height was set to zero; f) similar to e), but with our models for lapse rate and tropopause height (LA6). A comparative summary of the different Lanyi parameterizations is given in Table 2.

4. ANALYSIS AND CONCLUSIONS

The analysis of the performance of the different mapping functions is based on a comparison against ray tracing, for a full year of radiosonde soundings carried out at 50 stations distributed around the world and covering therefore a large variety of climatic conditions.

Table 2 – Different parameterization settings for the Lanyi mapping function (P - surface total pressure; T - surface (mean) temperature; RAOB - radiosonde observed values; SJ96 - interpolation scheme [Sove 96]; Mean - monthly mean values based on radiosonde observations; Model - tropopause height and lapse rate predicted by our models).

Version	P (hPa)	T (K)	α (K/km)	H _i (km)	H _t (km)
LA1	1013.25	292	6.8165	1.25	12.2
LA2	RAOB	SJ96	SJ96	0	SJ96
LA3	RAOB	RAOB	Mean	Mean	Mean
LA4	RAOB	Mean	Mean	Mean	Mean
LA5	RAOB	Mean	6.5	1.25	11.231
LA6	RAOB	Mean	Model	0	Model

Ray tracing was performed at different elevation angles, ranging from 3° to 30° (details on the ray tracing procedure can be found in Mendes and Langley [Mend 95]). For each elevation angle, a total of ~32 500 traces were generated. Fig. 3 shows the differences with respect to ray tracing for the different parameterizations of CfA and UNSW for the total delay at station Albany (New York) for an elevation angle of 10°.

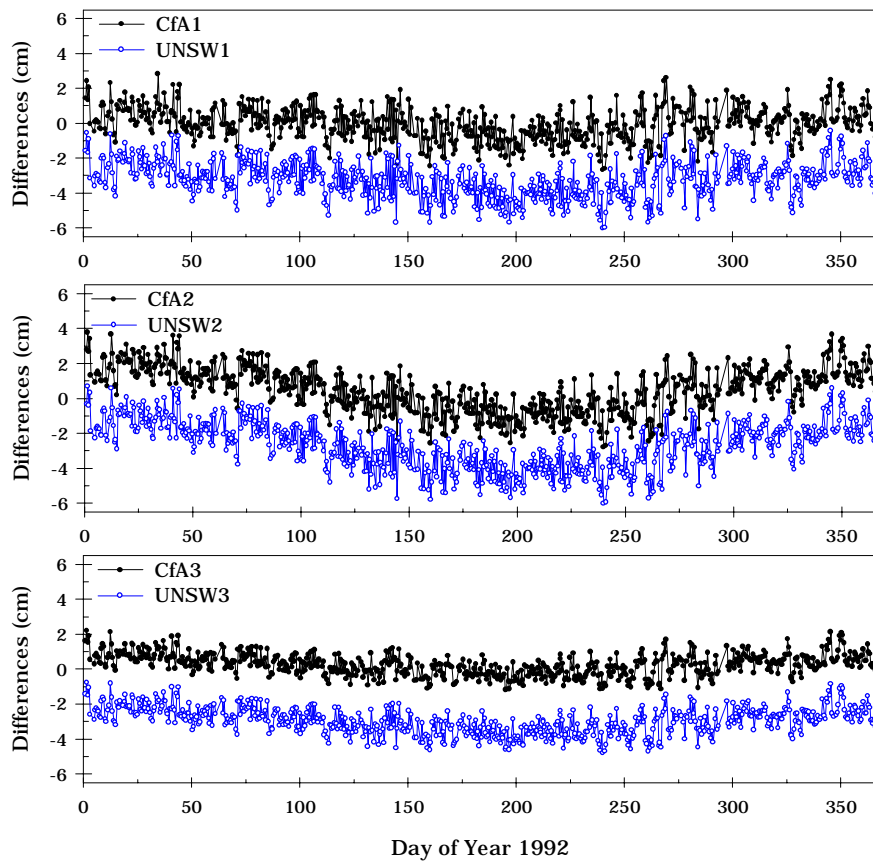


Fig. 3 – Differences between the total delay computed using the different parameterizations of CfA and UNSW and the ray-tracing results, at 10° elevation angle for Albany. A bias of -1 cm was added to UNSW values for the sake of clarity of the figure.

The first observation to be noted in examining these results is the high correlation between the two mapping functions (for all strategies), which is somewhat expected as CfA was used as basis for UNSW and they use the same input parameterization. The performance of these mapping functions is degraded when they are driven by nominal values, leaving a clear seasonal signature, especially for mid- and high-latitude stations. The elimination of this bias is not always very successful for the other two strategies, as illustrated in Fig. 4, which presents the results for the station Fairbanks (Alaska), for the same 10° elevation angle. This bias, or at least part of it, might be introduced by the use of the same mapping function in mapping both the hydrostatic and the wet zenith delay.

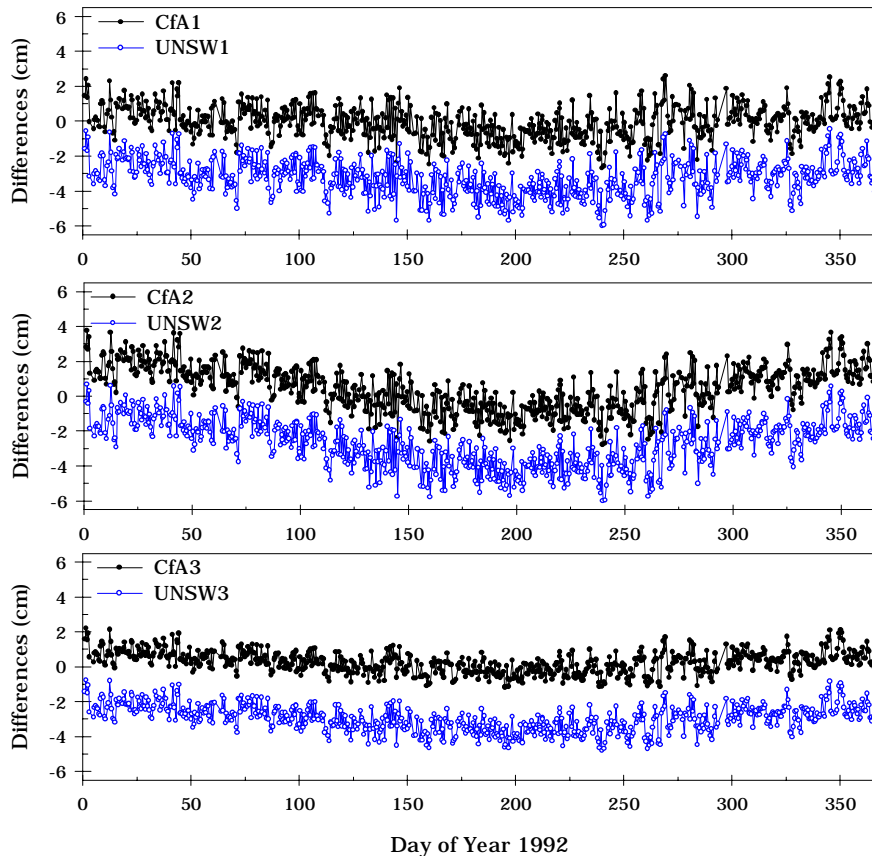


Fig. 4 – As Fig. 3, for Fairbanks. A bias of -1 cm was added to UNSW values for the sake of clarity of the figure.

As regards the r.m.s. scatter, there is a clear improvement, especially when our models are used (by a factor of about 2 as compared with CfA2/UNSW2, for many of the stations analyzed). If this fact is not surprising when compared to strategy CfA2/UNSW2, the significant improvement relative to CfA1/UNSW1 is very encouraging. The conclusions drawn from these illustrated case studies also apply to the other radiosonde stations, and are especially applicable in middle and high latitude regions.

The use of nominal values for tropopause height and temperature lapse rate, either using Lanyi's default values (LA1) or the values of 11.231 km and 6.5 K km^{-1} (LA5), also degrade the performance of Lanyi's mapping function. Fig. 5 shows the differences with respect to ray tracing for the different parameterization settings for the total delay at station Albany for 10° elevation angle.

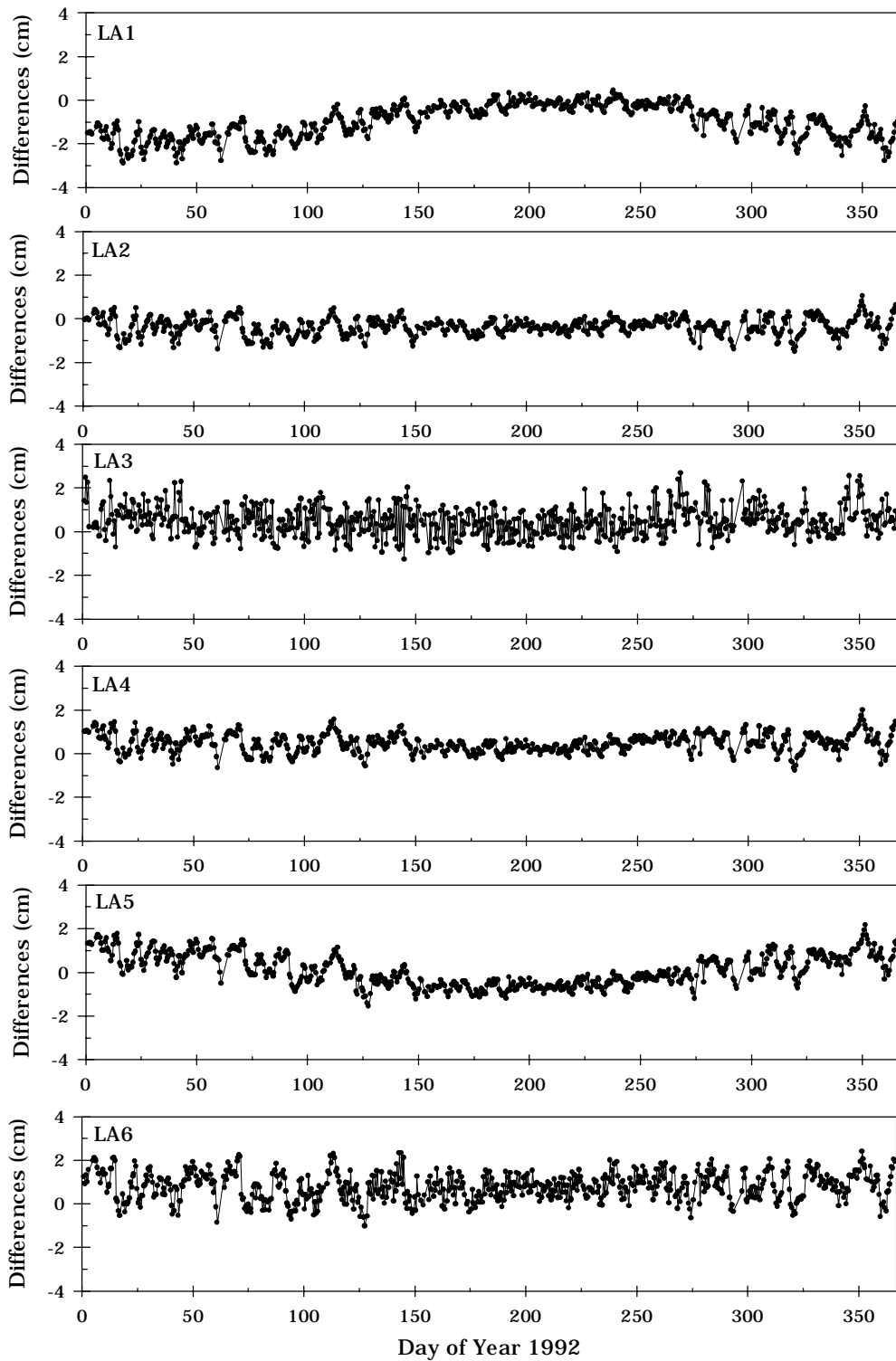


Fig. 5 – Differences between the total delay computed using the different parameterizations of Lanyi and the ray-tracing results at 10° elevation angle for Albany.

The best results are obtained using the interpolation scheme suggested by Sovers and Jacobs [Sove 96] (LA2). The use of the actual surface temperature (LA3) as alternative to using a mean temperature yields an increase in the r.m.s. scatter; when the actual surface temperature is replaced by the monthly means of our databases (LA4), the improvement in performance is significant. This fact may explain both the very good performance of Lanyi in low-latitude regions, which are characterized by very stable temperatures throughout the year, and the relatively bad performance

of the mapping function when driven by our models. Even though they have removed the seasonal trends existing in LA1 and LA5, the r.m.s. scatter is large compared with most of the other strategies. This behavior seems to indicate that we should probably also use the mean temperature values to drive our models, due to the high correlation of the temperature profile parameters with the surface temperature. In fact, when we adopt this strategy, we obtain a level of performance close to LA2, as shown in Fig. 6.

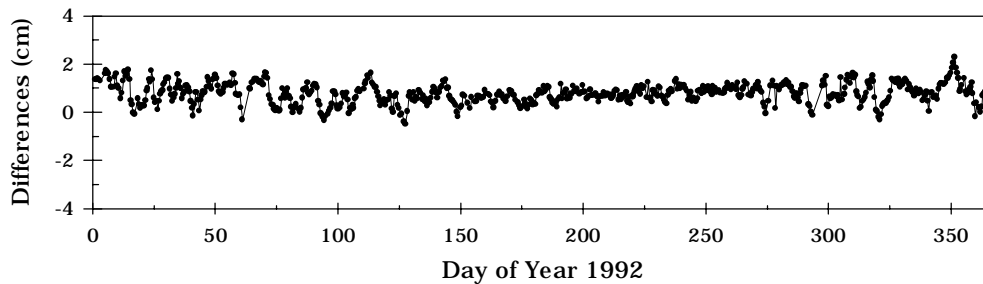


Figure 6 – As Fig. 5, for the Lanyi mapping function parameterized with predictions of tropopause height and lapse rate driven by monthly mean surface temperature (otherwise as LA6).

Another concern in Lanyi's parameterization should be the inversion height, as a change of 1 km in inversion height produces a change in Lanyi of -20 mm at a 6° elevation angle [Lany 84]. The effect is considerably greater than an equivalent change in tropopause height. The height of the top of the surface inversion layer is probably the most problematic parameter to be determined, due to its strong diurnal variation. The value suggested by Lanyi [Lany 84] seems to be too high for most locations, based on the analysis of our radiosonde database. On the other hand, similar and higher values were seen at arctic stations.

In summary, the use of nominal values in parameterization settings degrades the performance of all analyzed mapping functions. Our models for tropopause height and temperature lapse rate determination were able to improve significantly the performance of all models. As regards the mapping function developed by Lanyi, we concluded that our models should be driven by a mean temperature of the surface layer and not by the actual surface temperature, which increases the r.m.s. scatter.

REFERENCES:

- [Davi 85] J. L. Davis, T. A. Herring, I. I. Shapiro, A. E. E. Rogers, G. Elgered: "Geodesy by radio interferometry: Effects of atmospheric modeling errors on estimates of baseline length", *Radio Science*, Vol. 20, No. 6, pp. 1593-1607, 1985.
- [Envi 66] Environmental Science Services Administration, National Aeronautics and Space Administration, United States Air Force: *U.S. Standard Atmosphere Supplements, 1966*. U.S. Government Printing Office, Washington, D.C., 1966.
- [Hopf 69] H. S. Hopfield: "Two-quartic tropospheric refractivity profile for correcting satellite data", *Journal of Geophysical Research*, Vol. 74, No. 18, pp. 4487-4499, 1969.
- [Lany 84] G. Lanyi: "Tropospheric delay effects in radio interferometry", Jet Propulsion Laboratory, California Institute of Technology, Pasadena, Calif., TDA Progress Report No. 42-78, pp. 152-159, 1984.
- [Mari 72] J. W. Marini: "Correction of satellite tracking data for an arbitrary tropospheric profile", *Radio Science*, Vol. 7, No. 2, pp. 223-231, 1972.
- [Mend 95] V. B. Mendes, R. B. Langley: "Zenith wet tropospheric delay determination using prediction models: Accuracy analysis", *Cartografia e Cadastro*, No. 2, pp. 41-47, 1995.

- [Mend 98] V. B. Mendes: “Modeling the neutral-atmosphere propagation delay in radiometric space techniques”, Ph.D. dissertation (in preparation), Department of Geodesy and Geomatics Engineering, University of New Brunswick, Fredericton, New Brunswick, 1998.
- [Met91] Meteorological Office: *Meteorological Glossary*, HMSO Publications Centre, London, 1991.
- [Sove 96] O. J. Sovers, C. S. Jacobs: “Observation model and parameter partials for the JPL VLBI parameter estimation software “MODEST” – 1996”, JPL Publication 83-39, Rev. 6, Jet Propulsion Laboratory, California Institute of Technology, Pasadena, Calif., 1996.
- [Yanp 95] H. Yan, J. Ping: “The generator function method of the tropospheric refraction corrections”, *The Astronomical Journal*, Vol. 110, No. 2, pp. 934-939, 1995.